Numerical Investigation of Multiple Droplet Streams and the Effect on Grouping Behavior

Matthias Ibach*[1], Visakh Vaikuntanathan[2], Alumah Arad[3],
David Katoshevski[3], J. Barry Greenberg[4], Kathrin Schulte[1], Bernhard Weigand[1]

[1] Institute of Aerospace Thermodynamics (ITLR), University of Stuttgart, Stuttgart, Germany
[2]Department of Mechanical Engineering, Shiv Nadar University (SNU), UP, India
[3]Department of Civil and Environmental Engineering, Ben-Gurion University of the Negev (BGU), Beer-Sheva, Israel
[4]Aerospace Engineering, Technion – Israel Institute of Technology (IIT), Haifa, Israel
*Corresponding author: matthias.ibach@itlr.uni-stuttgart.de

Abstract

The exact knowledge of droplet clustering or grouping is important in many technical applications, such as fuel injection, ink-jet printing or in medical nebulizers. Despite their relevance, the fundamentals of grouping processes are yet to be fully understood. Recent studies comprise the experimental and numerical investigation of single monodisperse streams in well-defined droplet arrangements. Moving towards more complex configurations, such as multiple streams in close proximity, is a challenging task experimentally. This study aims at bridging this gap numerically with the aid of the in-house multiphase code Free Surface 3D to assess the effect of multiple droplet streams on grouping behavior. Three streams of droplets in a coplanar arrangement are simulated for which the center stream is compared to a single reference stream without the influence of neighboring droplets. To determine the impact of the outer streams on the center stream regarding grouping time, relative droplet velocity, drag forces as well as pressure and shear stress distribution, the following input parameters are changed systematically: the initial lateral distance to the center stream L_0 and the initial Reynolds number Re_0. Results show that the presence of neighboring streams with a lateral distance of $L_0/D \leq 5$ has a significant influence on the grouping behavior of the central stream. The process can be divided into a first part I where the outer streams confine the interaction with the surroundings, slowing down grouping tendencies and reducing drag forces in the middle stream; and a second part II where the coalescence of the outer streams imposes a substantial disturbance on the middle stream leading to an abrupt increase in the forces acting upon the droplets. Additionally, the lateral drift of the outside streams is compared qualitatively to literature studies and shows good agreement. For lateral distances of $L_0/D \geq 10$ the interaction of the streams is negligible and the behavior of a single, isolated stream is retained.

Keywords

CFD, DNS, VOF, droplet dynamics, droplet grouping, multiple streams, drag and lift forces

Introduction

The precise knowledge and manipulation of liquid spray characteristics in technical applications comprising fuel injection, pesticide control in agriculture, ink-jet printing or medical inhalators/nebulizers, is crucial for effective and safe use and operation. The dynamics of droplets is governed by the flow field around them, which in turn influences the motion of the droplets themselves. In real sprays and regions of large droplet concentration, the behavior can differ significantly from that of isolated droplets, which is often assumed to be the case for the sake of simplicity. Kim et al. [1] numerically investigated the three-dimensional flow over two identical spheres held fixed relative to each other and placed side by side. They computed lift, moment, and drag coefficients and investigated their dependence on the distance between the two spheres. The computations showed that the two spheres are repelled when the spacing is

of the order of the diameter but are weakly attracted at intermediate separation distances. The interaction of the wakes of two stationary spheres with the line connecting their centers normal to a uniform stream for Reynolds numbers between 200 and 350 was studied experimentally and with Direct Numerical Simulations (DNS) by Schouveiler et al. [2]. They observed distinctly different regimes of interaction, depending on the separation distance between the spheres. For medical applications, such as aerosol delivery through inhalation devices, nebulizers with vibrating membranes can be used, which produce parallel streams of droplets [3]. Here product performance depends highly on droplet size distribution, which can be altered by coagulation of droplets in the streams. Recently, Roth et al. [4] and Vaikuntanathan et al. [5] investigated experimentally single monodisperse droplet streams in well-defined droplet arrangements with precise boundary conditions. This very controllable system allows the study of basic effects and helps to provide insight into droplet-droplet interactions and involved mechanisms in streams. Observations revealed that slightly different inter-droplet spacings can lead to local *clustering* or *grouping* of initially distant droplets, which approach each other, coalesce and subsequently affect size, velocity and drag of the droplets.
Moving towards more complex configurations, such as multiple stable streams in coplanar arrangements in close proximity, is a challenging task experimentally and grouping in parallel streams has not been investigated in detail yet. For this reason, we numerically investigate the influence of multiple droplet streams and the effect on grouping behavior by using our in-house multiphase flow solver Free Surface 3D (FS3D), which is described in more detail in the following section. The extension of the computational setup based on previous studies of Ibach et al. [6] to three streams of droplets in line along one common plane is presented afterwards, along with details on the operating conditions and relevant parameters. To determine the impact of the outer streams on the center stream regarding grouping time, relative droplet velocity as well as involved drag and lift forces, the following input parameters are varied systematically: the initial lateral distance to the center stream L_0 and the initial Reynolds number Re_0. The results are compared to a reference case consisting of a single, isolated stream. Finally, the work is summarized and concluded.

Fundamentals

Numerical Method

The ITLR in-house multiphase flow solver FS3D is employed for the conducted grouping simulations at hand. The code allows for Direct Numerical Simulation of incompressible multiphase flows with sharp interfaces between the phases. The underlying conservation equations are discretized by finite volumes in space on a Cartesian staggered grid arrangement and read

$$\partial_t \rho + \nabla \cdot (\rho \mathbf{u}) = 0 \tag{1}$$

for the mass conservation and

$$\partial_t (\rho \mathbf{u}) + \nabla \cdot [(\rho \mathbf{u}) \otimes \mathbf{u}] = \nabla \cdot [\mathbf{S} - \mathbf{I}p] + \rho \mathbf{g} + \mathbf{f}_\sigma \tag{2}$$

for the momentum conservation with t denoting the time, ρ the density, $\mathbf{u}$ the velocity vector, $\mathbf{I}$ the identity matrix and p the pressure. The shear stress tensor $\mathbf{S}$ is defined as $\mathbf{S} = \mu[\nabla \mathbf{u} + \nabla \mathbf{u}^T]$ with μ representing the dynamic viscosity for the assumed Newtonian fluid. Other body forces, such as gravity or surface tension, are represented by $\mathbf{g}$ and $\mathbf{f}_\sigma$, respectively, where the latter term is modeled by the Continuum Surface Stress (CSS) model of Lafaurie et al. [7]. FS3D employs the Volume-of-Fluid (VOF) method according to Hirt and Nichols [8] to distinguish between the two different phases, in this work a liquid (subscript l) and a gaseous phase (subscript g). Therefore, an additional scalar field $f(\mathbf{x}, t)$ representing the liquid volume fraction in a computational cell is introduced. The scalar is defined as 0 in the gaseous phase, 1 in the liquid phase and is taking values between $(0, 1)$ indicating the presence of an interface inside a computational cell. The spatial and temporal evolution of the interface is calculated by an additional transport equation

$$\partial_t f + \nabla \cdot (f \mathbf{u}) = 0. \tag{3}$$

To keep the interface sharp and reduce numerical diffusion, FS3D makes use of the Piecewise Linear Interface Calculation (PLIC) algorithm, following the formulation of Rider and Kothe [9]. The dilatation term, which results due to the employed directional operator-split technique of Eq. (3), is treated as suggested by Weymouth and Yue [10] to ensure complete volume conservation during the advection of the scalar $f(\mathbf{x}, t)$. The flow field is calculated by solving Eqs. (1) and (2) in a one-field formulation where physical properties φ, such as the density ρ, are expressed locally as

$$\varphi(\mathbf{x}, t) = \varphi_g(1 - f(\mathbf{x}, t)) + \varphi_l f(\mathbf{x}, t). \tag{4}$$

Due to the very fine discretization of the problem both temporally and spatially, FS3D is parallelized using MPI as well as OpenMP and is adapted to efficiently run on the HPE Apollo supercomputer "Hawk" at the High Performance Computing Center Stuttgart (HLRS) where all presented simulations were performed. The code was further optimized by implementing a Connected Component Labeling (CCL) algorithm to extract relevant droplet information (see below section *Operating Conditions and Relevant Parameters*) efficiently from the simulation already during runtime [11]. For a more detailed overview on Free Surface 3D and its capabilities, the reader is referred to Eisenschmidt et al. [12].

Computational Setup

The computational setup for the simulation of multiple droplet streams is similar to the one presented by Ibach et al. [6] for the case of single streams and is depicted in Fig. 1. Four droplets with diameter D and initial velocity V_0 are placed in the center of the computational domain along a common center line with the gravitational force $\mathbf{g} = \begin{pmatrix} 9.81 & 0 & 0 \end{pmatrix}^T$ [m s^{-2}] pointing in the direction of droplet motion. This setup, indicated by the dashed lines in the figure, is used as the reference case, which represents a single, isolated stream. To investigate the effect of other streams in proximity of the reference stream, two additional streams are placed along the center of the y-axis with a distance of $\pm L_0$ resulting in a coplanar arrangement. This setup allows for a good comparison with the possibility of directly comparing it to the reference case of an isolated stream. Furthermore, the setup can be easily extended to account for more complex arrangements and well-defined experimental investigations are still feasible. Two slightly different spacings $a_{1,0}$ and $a_{2,0}$ within a stream are instantiated to create two pairs of droplets. The different inter-droplet spacings indicate the distance between the last droplet of a pair and

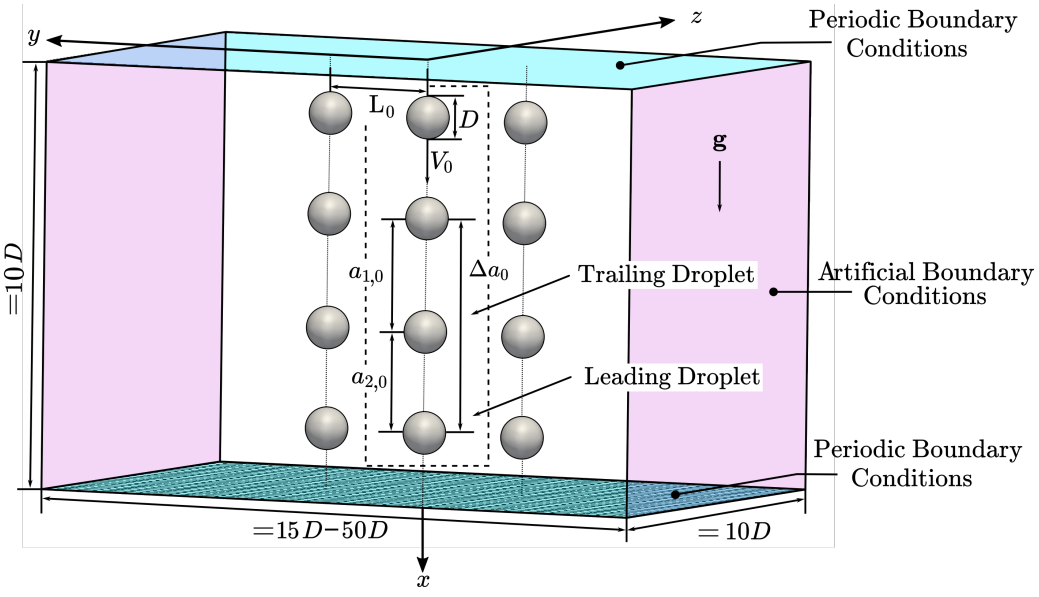

Figure 1. Computational setup of three droplet streams with initial lateral distance of L_0 in an equidistant grid (depicted on bottom), the reference single stream is marked with a dashed rectangle. Periodic boundary conditions are applied in direction of droplet motion (light blue), artificial boundary conditions are used for all remaining sides (light magenta).

the first droplet of the following pair a_1 and the spacing between the droplets of a single pair a_2. The distance between a droplet group is defined as $\Delta a_0 = a_{1,0} + a_{2,0}$. In the course of this work, the terms *leading* and *trailing* droplet are used in reference for the droplets within a group, as shown in Fig. 1. The computational domain is discretized using a regular Cartesian grid with a distance of the domain boundaries in x- and z-direction of $10D$ without the use of symmetry conditions for all cases. The droplets are resolved with ≈ 26 grid cells per droplet diameter, which is in accordance with previous numerical work [6]. The extension of the domain in the lateral y-direction is dependent on the simulated case, i.e., the lateral distance L_0 of the outer streams to the central stream. The grid resolution therefore varies between $256 \times 256 \times 256$ and $256 \times 256 \times 1280$ computational cells, determined by the investigated setup. Periodic boundaries are applied in the direction of droplet motion (see light blue boundaries) to mimic the behavior of a continuous stream in direction of droplet motion. All remaining boundaries are Artificial Boundary Conditions (ABCs, light magenta boundaries) according to Ibach et al. [6]. The ABCs guarantee stability of the droplet stream and more realistic approximation of the free stream without influencing the physical behavior of droplet grouping.

Operating Conditions and Relevant Parameters

The material properties of the liquid phase and the surrounding gaseous environment correspond to the experimental investigations of monodisperse streams conducted at the ITLR droplet grouping test rig (see in more detail [4, 5]) and are set for iso-propanol droplets at ambient pressure and temperature of $294.95\mathrm{K}$. The initial diameter and velocities are equal for all droplets in the computational domain for the sake of simplicity. For the numerical study, only the initial droplet velocity and the initial lateral distance of the streams are varied as these are the parameters used to quantify the effect of multiple streams on grouping behavior. Important nondimensional numbers comprise the initial Reynolds number in the stream $Re_0 = \rho_g V_0 D/\mu_g$, the initial aerodynamic Weber number $We_0 = \rho_g V_0^2 D/\sigma$ along with the Ohnesorge number $Oh = \mu_l/\sqrt{\rho_l \sigma D}$, where the subscript 0 symbolizes initial values or conditions. Furthermore, geometrical dimensions are defined, e.g. the initial inter-droplet separation between two droplets within a group $a_{2,0}/D$, the group distance $\Delta a_0/D$ or L_0/D as the initial lateral distance of the outer streams to the reference stream, all nondimensionalized by the droplet diameter D. The corresponding investigated ranges of these parameters for this numerical study as well as relevant material properties and operating conditions are given in Table 1. To quantify the effect of multiple streams on grouping behavior, the following parameters are investigated in more detail. The temporal and spatial evolution of the nondimensional inter-droplet spacings a_1/D and a_2/D can be directly compared to experimental data and are important for validation purposes. The grouping time Δt_{gr} until leading and trailing droplet within a group coalesce/merge and the relative velocity at that time instant ΔV_{gr} are examined as well. The subscript gr indicates the moment the droplets come into contact for the first time after being apart initially. With the presence of multiple streams, the lateral drift of the outer streams $\Delta L/D$ is directly assessed. Drag and lift forces or the corresponding nondimensional coefficients play a vital role in the motion, the trajectory, final settling points or the impact velocity of droplets in streams or sprays. Therefore, these quantities are computed for each droplet in the

Table 1. Fluid properties of iso-propanol and air at ambient pressure ($p = 1$ atm) and temperature of $294.95\mathrm{K}$ following experimental studies of [4, 5] along with operating conditions as well as relevant geometrical dimensions and grid resolution.

Fluid properties					Operating conditions		
ρ_l	ρ_g	μ_l	μ_g	σ	Re_0	We_0	Oh
$\mathrm{kg\,m^{-3}}$	$\mathrm{kg\,m^{-3}}$	$\mathrm{mPa\,s}$	$\mathrm{mPa\,s}$	$\mathrm{mN\,m^{-1}}$	$-$	$-$	$-$
784.5	1.197	2.265	0.01829	21.28	$300 - 500$	$5.009 - 13.91$	0.03608
Geometrical dimensions					Grid resolution		
$a_{1,0}/D$	$a_{2,0}/D$	$a_{1,0}/a_{2,0}$	$\Delta a_0/D$	L_0/D	$Computational\ cells$		
$-$	$-$	$-$	$-$	$-$	$-$		
2.65	2.35	1.128	5.0	$1.5 - 20$	$256 \times 256 \times 256 - 256 \times 256 \times 1280$		

stream with the aid of the highly resolved velocity and pressure fields available from the DNS. Therefore, the code framework of FS3D was extended to calculate the contributions of viscous and pressure drag and lift acting on each droplet in the stream. The general formulation of the drag force F_D and the lift force F_L is defined as

$$F_{\{D,L\}1,2} = \int_{A_{1,2}} \underbrace{\mathbf{n_{1,2}} \cdot \mathbf{S} \cdot \{\mathbf{i},\mathbf{k}\} dA_{1,2}}_{F_{\{D,L\}\tau 1,2}} + \int_{A_{1,2}} \underbrace{-p_{1,2}\mathbf{n_{1,2}} \cdot \{\mathbf{i},\mathbf{k}\} dA_{1,2}}_{F_{\{D,L\}p1,2}} \tag{5}$$

where $A_{1,2}$ is the surface area of the droplets, $\mathbf{n_{1,2}}$ is the outward unit normal vector at the surface, $\mathbf{i}$ is the unit vector in x-direction (which is the direction of droplet motion) for the drag force $F_{D1,2}$ and $\mathbf{k}$ denotes the unit vector in y-direction (which is the direction of droplet motion laterally) for the lift force $F_{L1,2}$, $p_{1,2}$ is the pressure at the droplet surface and $\mathbf{S}$ is the surface stress tensor, with the subscripts 1 and 2 representing the leading and the trailing droplets, respectively. The first term of Eq. (5) describes the contribution to the drag or lift force due to viscous effects, whereas the second term stands for the pressure drag contribution to either force. The drag and lift forces $F_{\{D,L\}1,2}$ may be represented in a nondimensional form by

$$c_{\{D,L\}1,2} = \frac{F_{\{D,L\}1,2}}{(\rho_g/2)V_{1,2}^2 A_{pr1,2}} \tag{6}$$

with $A_{pr1,2}$ being the area of the droplet projected onto a plane perpendicular to the flow direction. Along with the nondimensionalization in Eq. (6), the distinction between viscous and pressure drag allows for a study of the relative importance of both contributions $c_{\{D,L\}p1,2}/c_{\{D,L\}\tau 1,2}$ at different operating conditions. In the following section, the aforementioned parameters are evaluated to characterize the influence of multiple droplet streams on the grouping behavior after introducing the isolated, single stream reference case briefly at first.

Results and Discussion

A reference case of a single, isolated droplet stream is chosen as the basis to quantify the effect of neighboring streams on relevant parameters of grouping. The numerical setup is based on experiments conducted at the ITLR droplet grouping test rig with similar initial geometrical dimensions $a_{1,0}$, $a_{2,0}$ and Δa_0. This setup is indicated with the dashed rectangle in Fig. 1. In the following plots, the results of the baseline case are always indicated in black dashed lines. The reference values of grouping time Δt_{gr}, approach velocity ΔV_{gr} as well as drag and lift coefficients $c_{\{D,L\}i}$ are given in Table 2 in the top row of each case.

Figure 2 shows an exemplary case at $Re_0 = 300$ of three droplet streams arranged in line with an initial lateral separation of $L_0/D = 2$. The snapshot at $t = 6.2\mathrm{ms}$ depicts the velocity magnitude of the flow field in the reference system of the trailing droplet along with streamlines colored by the vorticity magnitude. The center stream appears to be more isolated from the free flow due to the presence of the neighboring streams, made visible through the surface shear stress plotted on the droplet contours via grayscale colors and the isolines of the normalized pressure coefficient $c_{p,n} = 2p/(\rho_g V_2^2)$. This fact becomes more evident when comparing the leading and trailing droplet velocities $V_{1,2}$ and drag coefficients $c_{D1,2} = c_{Dp1,2} + c_{D\tau 1,2}$ to the reference case. The evolution of the droplet's velocities over the nondimensional inter-droplet separation for the case with multiple streams can be divided into two parts. In the first part I, the outer streams confine the interaction with the surroundings, slowing down the decrease of the leading and trailing droplet's velocity and therefore decreasing grouping tendencies of the middle stream, see Fig. 3(a). The second part II reveals a substantial disturbance imposed by the coalescence of the outer streams, which leads to a faster droplet approach and collision velocity ΔV_{gr}. Furthermore, the absolute velocities of leading and trailing droplet V_1 and V_2 are below the values of the reference case, indicating an increase in drag acting upon the droplets. Note that the graphs have to be read from right to left moving from the initial separation $a_{2,0}/D = 2.35$ towards decreasing a_2/D with droplet coalescence at $a_2/D = 1$, indicated

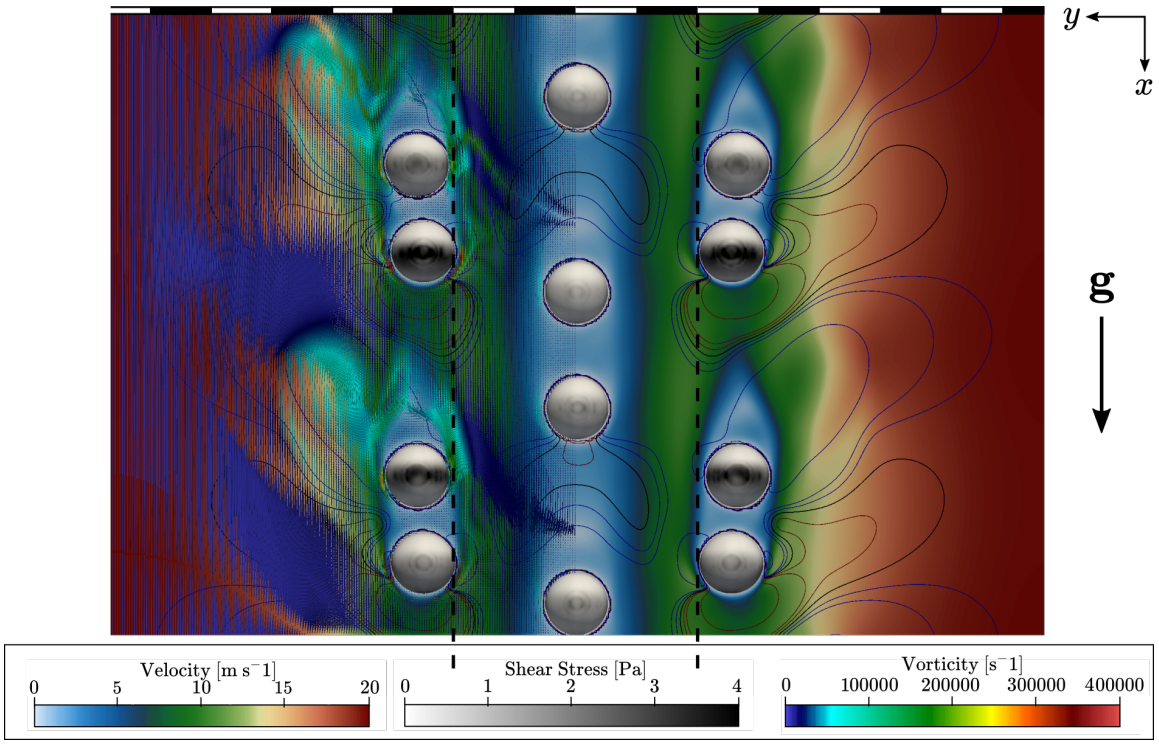

Figure 2. Snapshot of droplet grouping with multiple streams in a coplanar arrangement at $t = 6.2\text{ms}$. Visualization of velocity magnitude in the reference system of the trailing droplet along with streamlines colored in the vorticity magnitude (left half), shear stress plotted on the droplet contours and iso-lines of the pressure coefficient (red: $c_{p,n} > 0$, blue: $c_{p,n} < 0$, black: $c_{p,n} = 0$).

by the vertical blue line. A similar behavior of the center stream is observable for the drag coefficients, depicted in Fig. 3(b). In the initial stage I (before the outer streams group), the drag coefficients c_{D1} and c_{D2} are generally below the reference case of an isolated stream. Upon the coalescence of the droplets from the neighboring streams (occurring at a comparable time span as the reference case), a strong perturbation on the flow field is introduced resulting in an abrupt increase in drag forces acting on the center stream in the later stage II, before falling again at $a_2/D \lesssim 1.3$.

Taking into account varying initial Reynolds numbers Re_0 and lateral separation L_0/D, the grouping process of the central and outer streams still resembles the case of an isolated stream. With progressing time, two pairs of droplets form with the trailing droplet eventually catching up

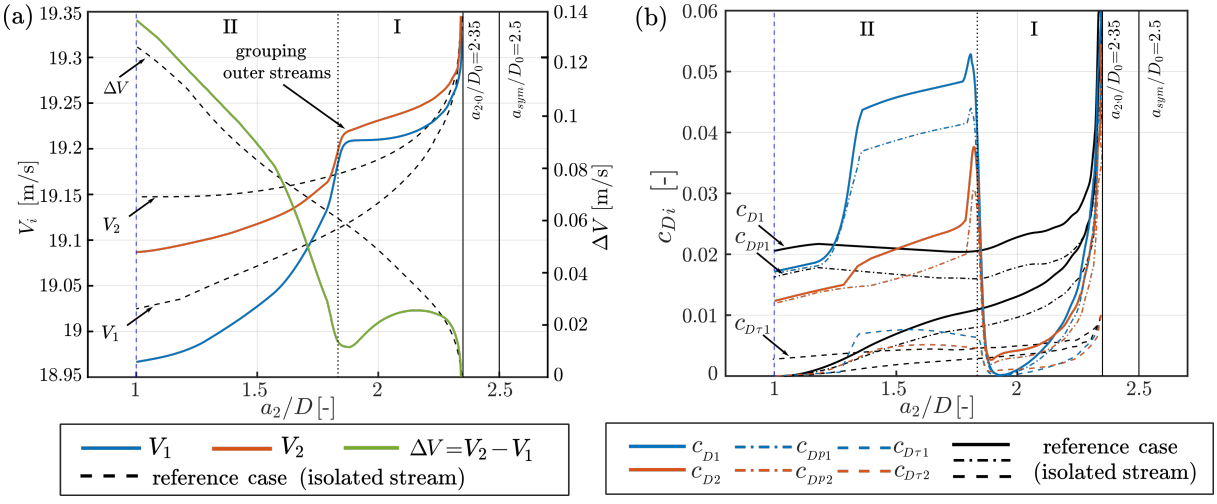

Figure 3. (a) Absolute velocity V_1, V_2 and relative velocity ΔV of leading and trailing droplet over nondimensional inter-droplet distance a_2/D for the central stream. (b) Drag coefficient of leading and trailing droplet c_{D12}, c_{D2} over a_2/D. The shown exemplary case is $Re_0 = 300$ at $L_0/D = 2$. Dashed black lines indicate values of the reference case (isolated, single stream).

to the leading droplet within a pair, resulting in a merging/coalescence to two larger droplets. Slightly upon coalescence, a tilting of the droplets in the outer stream is observable (see Fig. 2). However, the process of droplet grouping happens faster for the outer streams than for the central stream. The presence of the outer streams isolate the central stream eventually leading to a more than 55% longer time until grouping for the inner stream and even a $\approx 28\%$ longer Δt_{gr} for the outer stream at $L_0/D = 1.5$ and $Re_0 = 300$, see Fig. 4(a). An influence on the grouping time (marked with an asterisk $*$) is discernible for an initial lateral distance of $L_0/D < 10$ and is more pronounced for the lowest investigated Reynolds number $Re_0 = 300$ (in yellow) than for $Re_0 = 400$ (in purple) and $Re_0 = 500$ (in cyan). The same is true for the collision velocities, which are plotted on the right y-axis (depicted with a cross symbol $\times$). The trend of ΔV_{gr} shows a somewhat non-monotonic dependence on the initial lateral distance L_0/D. Taking the case at $Re_0 = 500$ (cyan $\times$) as an example, a peak at $L_0/D = 2$ of $\Delta V_{gr} = 0.3131\,\mathrm{m\,s^{-1}}$ is apparent, which means a collision velocity that is approximately 42% higher than for the reference case. With larger initial lateral separation of the outer streams, the approach velocity decreases continuously reaching the values of the isolated stream at $L_0/D \geq 10$ for all investigated cases. At this point, there is no interaction of the outer streams with the central stream anymore and an isolated behavior of each stream is evident. The values of the reference case are depicted with a solid line for comparison, intercepting the y-axis on the left for Δt_{gr} and on the right for ΔV_{gr}. Note that for the sake of clarity the initial lateral distance on the x-axis is plotted on a logarithmic scale.

Although it is evident that there is a strong local and temporal dependence of the drag forces acting upon the droplets within the stream, it is practical to define average values for the total drag coefficients $\overline{c}_{D1,2}$ or the ratio of pressure to shear drag $\overline{c}_{p1,2}/\overline{c}_{\tau 1,2}$. The averaging for this study is conducted by taking a simple arithmetic mean value for the entire grouping process until Δt_{gr}. For the sake of simplicity, Fig. 4(b) depicts the average drag coefficient $\overline{c}_{D2}$ (diamond symbols $\diamond$) for the trailing droplet at different initial lateral distances of the outer stream and different initial Reynolds numbers. In general, the drag coefficients for the trailing droplet are higher for the cases with multiple droplet streams than for the isolated reference stream case. This is interesting since in the initial stage of the grouping process I the drag coefficient is lower than for the isolated case. The abrupt increase of c_{D2} after the coalescence of the outer streams in the second part II of the grouping process is substantially higher, leading to higher average values of the drag coefficient. This trend is also observable for the leading droplet, with slightly higher absolute values for c_{D1} and $\overline{c}_{D1}$, although not depicted here explicitly. The investigation of the pressure to shear drag ratio $\overline{c}_{p1,2}/\overline{c}_{\tau 1,2}$ shows that the pressure is the main contributor to

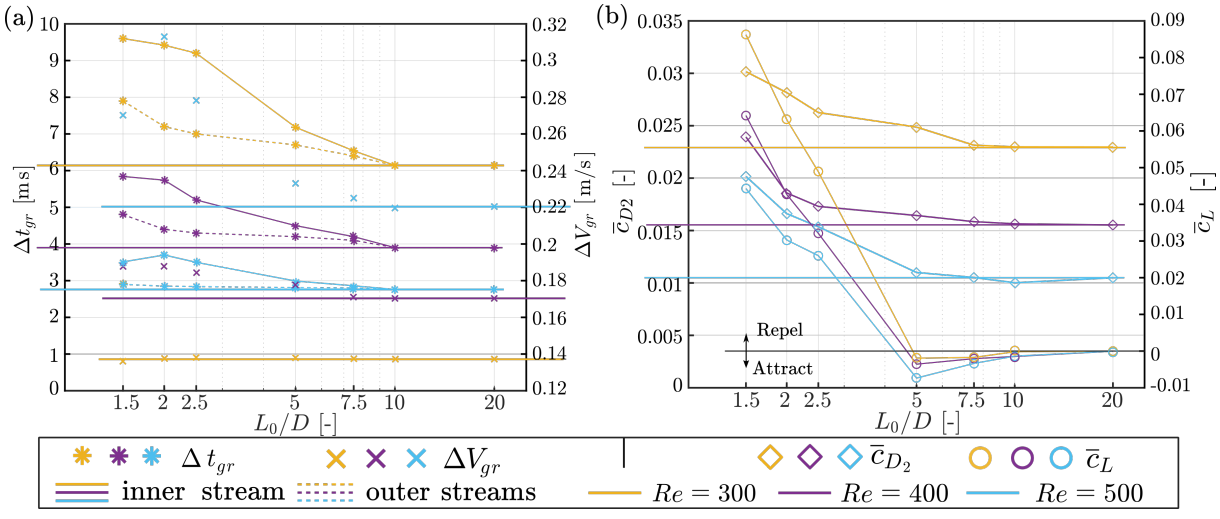

Figure 4. (a) Grouping time Δt_{gr} and velocity upon droplet coalescence ΔV_{gr} for inner stream and outer streams over initial lateral distance L_0/D at different Re_0. (b) Averaged drag coefficient of trailing droplet $\overline{c}_{D2}$ and lift coefficient of outer streams $\overline{c}_L$ over L_0/D at different Re_0. Solid lines indicate values of the reference case (isolated, single stream).

the drag force for all studies. The larger the Reynolds number, the higher the pressure effect, i.e., an increasing pressure to shear drag ratio. Exemplary results for $L_0/D = 2$ are given in Table 2. It is worth pointing out the fact that even if multiple streams are involved, the ratio was always similar to the reference case for all investigated initial separation distances. The highest observed deviation of $\overline{c}_{p1,2}/\overline{c}_{\tau 1,2}$ was $\approx 8\%$ at $Re_0 = 500$ and $L_0/D = 2$.

As mentioned before, the grouping process of the outer streams is similar to the reference case of a single stream with the difference of a lateral movement of the entire stream. Figure 2 shows the initial position of the outer streams with a vertical dashed line. Using the black and white scale on top of the figure, it is easy to track the sideways movement of the stream away from the central stream, in this case after $t = 6.2\mathrm{ms}$. This movement is characterized with the averaged lift coefficient $\overline{c}_L$. In this case, the value of $\overline{c}_L$ is representative for the entire outer streams as the values for $\overline{c}_{L1,2}$ for leading and trailing droplets of the left and the right stream are almost identical. Figure 4(b) shows the total lift coefficient on the right y-axis plotted against L_0/D for different Reynolds numbers (marked as circles $\circ$). The lift coefficient $\overline{c}_L$ is highest when the streams are close and decreases for increasing initial lateral distance. The positive value indicates that the streams repel each other and that the repulsion is stronger the closer they are. Additionally, higher initial Reynolds numbers decrease the lift coefficient. The lateral displacement $\Delta L_{gr}/D$ of the outer streams just at the moment when the reference stream groups, increases with increasing Reynolds numbers. This is exemplarily depicted in the last column of Table 2 for $L_0/D = 2$. The final lateral distance increases from $\Delta L_{gr} \approx 0.57D$ for $Re_0 = 300$ up to $\Delta L_{gr} \approx 0.91D$ for $Re_0 = 500$. For $L_0/D \geq 5$ the lift coefficient is negative which implies that the streams attract each other weakly causing a movement of the outer streams towards the central stream. These general trends are in accordance with findings reported in literature, e.g. by Kim et al. [1], who investigated Reynolds numbers of $50-150$. For $L_0/D \geq 10$, the lift vanishes and the streams have no interactions at any Reynolds numbers.

Table 2. Results for grouping time Δt_{gr}, velocity upon droplet coalescence ΔV_{gr}, averaged drag coefficients $\overline{c}_{D1,2}$, pressure to shear drag ratio $\overline{c}_{p1,2}/\overline{c}_{\tau 1,2}$, lift coefficient $\overline{c}_L$ and lateral movement of outer streams $\Delta L_{gr}/D$ at the moment when the reference stream groups. The top row of each Re_0-case depicts the results of the reference case (isolated stream), the bottom row shows the exemplary case at $L_0/D = 2$. The results in the brackets for Δt_{gr} depict the grouping time of the outer streams.

	Δt_{gr} ms	ΔV_{gr} $\mathrm{m\,s^{-1}}$	$\overline{c}_{D1}$ –	$\overline{c}_{D2}$ –	$\overline{c}_{p1}/\overline{c}_{\tau 1}$ –	$\overline{c}_{p2}/\overline{c}_{\tau 2}$ –	$\overline{c}_L$ –	$\Delta L_{gr}/D$ –
$Re_0 = 300$ *Ref.*	*6.1*	*0.1246*	*0.02926*	*0.02292*	*4.037*	*3.136*		
$L_0/D=2$	9.4 (7.2)	0.1375	0.03103	0.02816	3.942	3.207	0.06310	0.5738
$Re_0 = 400$ *Ref.*	*3.9*	*0.1704*	*0.02339*	*0.01554*	*4.808*	*3.615*		
$L_0/D=2$	8.7 (4.4)	0.1916	0.02847	0.01859	5.008	3.977	0.0427	0.6310
$Re_0 = 500$ *Ref.*	*2.8*	*0.2204*	*0.01901*	*0.01050*	*5.744*	*4.125*		
$L_0/D=2$	3.7 (2.9)	0.3131	0.02207	0.01661	6.193	4.445	0.03029	0.9122

Conclusions

In this study, we numerically investigated the effect of multiple droplet streams on grouping behavior with the multiphase DNS code FS3D. To evaluate the influence of neighboring streams, the initial lateral separation distance L_0 was varied between $1.5-20$ droplet diameters for initial Reynolds numbers of $Re_0 = 300-500$. Relevant parameters to quantify the outcome are selected to be the time until grouping Δt_{gr}, the velocity upon droplet coalescence ΔV_{gr}, averaged drag coefficients $\overline{c}_{D1,2}$, the pressure to shear drag ratio $\overline{c}_{p1,2}/\overline{c}_{\tau 1,2}$, the lift coefficient $\overline{c}_L$ and the lateral movement of the outer streams $\Delta L_{gr}/D$ at the moment when the reference stream groups. The results of these parameters were evaluated for the central stream and directly compared to a reference case of a single, isolated droplet stream.

In general, the grouping process of multiple streams in coplanar arrangement resembles the case of an isolated, single stream. For initial lateral separation of $L_0/D \leq 5$ the grouping behavior differs and can be divided into a first part I where the presence of the outer streams confines the interaction of the central stream with the surroundings. This leads to a slower decrease in velocity and lower drag coefficients for the droplets in the stream, decreasing grouping ten-

dencies. The strong perturbation on the flow field initiated by the coalescence of the droplets from the neighboring streams leads to an abrupt increase of drag forces acting on the center stream, marked as stage II. These effects are reflected in up to $\approx 55\%$ longer grouping times and $\approx 42\%$ higher relative velocities upon droplet coalescence. The lateral drift of the outer streams increases with higher initial Reynolds number and reaches up to $\Delta L_{gr}/D = 0.9122$ at the instant when the reference stream groups. For $L_0/D \geq 5$ the lift coefficient becomes negative which implies that the streams attract each other. For initial lateral distances of more than ten droplet diameters, no interaction of the streams is discernible anymore and all investigated parameters retain the values of the single, isolated reference droplet stream.

Acknowledgements

This work is funded by the Deutsche Forschungsgemeinschaft (DFG, German Research Foundation) under Germany's Excellence Strategy - EXC 2075 – 390740016. We also acknowledge the support by the Stuttgart Center for Simulation Science (SimTech). Furthermore, the authors kindly acknowledge the High Performance Computing Center Stuttgart (HLRS) for the support and the supply of computational resources on the HPE Apollo (Hawk) platform under the Grant No. FS3D/11142 and the financial support of DFG through the project 'Investigation of Droplet Motion and Grouping' (project number 409029509).

References

[1] Kim, I., Elghobashi, S., Sirignano, W. A., 1993, *J. Fluid Mech.*, 246, pp. 465-488.
[2] Schouveiler, L., Brydon, A.,Leweke, T., Thompson, M.C., 2004, *Eur. J. Mech. B Fluids*, 23 (1), pp. 137-145.
[3] Li, Z., Perkins, W., Cipolla, D., 2021, *Eur. J. Pharm. Biopharm.*, 166, pp. 10-18.
[4] Roth, N., Gomaa, H., Livne, A., Katoshevski, D., Weigand, B., 6-8 Sep. 2017, 28th ILASS 2017, Valencia, Spain.
[5] Vaikuntanathan, V., Amini, K., Arad, A., Katoshevski, D., Greenberg, J.B., Weigand,B., 29 Aug.-2 Sept. 2021, 15th Triennial ICLASS 2021, Edinburgh, UK.
[6] Ibach, M., Schulte, K., Vaikuntanathan, V., Arad, A., Katoshevski, D., Greenberg, J.B., Weigand, B., 29 Aug.-2 Sept. 2021, 15th Triennial ICLASS 2021, Edinburgh, UK.
[7] Lafaurie, B., Nardone, C., Scardovelli, R., Zaleski, S., Zanetti, G., 1994, *J. Comput. Phys.*, 113 (1), pp. 134-147.
[8] Hirt, C.W. and Nichols, B.D., 1981, *J. Comput. Phys.*, 39 (1), pp. 201-225.
[9] Rider, W. J. and Kothe, D. B., 1998, *J. Comput. Phys.*, 141 (2), pp. 112-152.
[10] Weymouth, G.D. and Yue, Dick K.-P., 2010, *J. Comput. Phys.*, 229 (8), pp. 2853-2865.
[11] Schlottke, A., Ibach, M., Steigerwald, J., Weigand, B., 2022, 'High Performance Computing in Science and Engineering '21' (accepted), Springer Cham.
[12] Eisenschmidt, K., Ertl, M., Gomaa, H., Kieffer-Roth, C., Meister, C., Rauschenberger, P., Reitzle, M., Schlottke, K., Weigand, B., 2016, *Appl. Math. a. Comp.*, 272 (2), pp. 508-517.